REPORT DOCUMENTATION PAGE

AFRL-SR-AR-TR-08-0222

1. REPORT DATE *(DD-MM-YYYY)*	2. REPORT TYPE	3. DATES COVERED *(From - To)*
04-04-2008	Final Progress Report	Mar 2004-Feb 2007

4. TITLE AND SUBTITLE

FUNDAMENTAL ELECTRONIC STRUCTURE CHARACTERISTICS AND MECHANICAL BEHAVIOR OF AEROSPACE MATERIALS

5a. CONTRACT NUMBER

5b. GRANT NUMBER
FA9550-04-01-0013

5c. PROGRAM ELEMENT NUMBER

6. AUTHOR(S)

Freeman, Arthur, J.; Kontsevoi, Oleg, Y.; Gornostyrev, Yuri, N.; Medvedeva Nadezhda, I.

5d. PROJECT NUMBER

5e. TASK NUMBER

5f. WORK UNIT NUMBER

7. PERFORMING ORGANIZATION NAME(S) AND ADDRESS(ES)

Northwestern University
Dept. of Physics & Astronomy
2145 N. Sheridan Rd.
Evanston, IL 60208-3112

8. PERFORMING ORGANIZATION REPORT NUMBER

9. SPONSORING / MONITORING AGENCY NAME(S) AND ADDRESS(ES)

Air Force Office of Scientific Research
875 N. Randolf St. Suite 325
Arlington, VA 22203-1768

10. SPONSOR/MONITOR'S ACRONYM(S)
AFOSR

11. SPONSOR/MONITOR'S REPORT NUMBER(S)

Dr Victor Giurgiutiu/NA

12. DISTRIBUTION / AVAILABILITY STATEMENT

Approved for public release; distribution is unlimited

13. SUPPLEMENTARY NOTES

20080502074

14. ABSTRACT

To fulfill the great potential of intermetallic alloys for high temperature structural applications, it is essential to understand the mechanisms controlling their mechanical behavior on the microscopic level. We focus on the mechanical behavior of homogeneous intermetallics with $L1_2$ and B2 structures, two-phase γ/γ' alloys, and *bcc* transition metals and their alloys. Based on highly-accurate total energy calculations and large-scale Peierls-Nabarro and atomistic modeling, we investigated the relation between electronic structure, dislocation properties, and brittle-ductile behavior in these metals and alloys. We demonstrated that Ir- and Rh-based alloys are intrinsically brittle and established the dislocation structure in Ir and Rh-based $L1_2$ alloys. We determined the temperature dependence of the lattice misfit parameter in γ/γ' superalloys, and established its simple relation with the alloy phase diagram. We studied the structure of dislocations in bcc Nb, Ta, Mo and W alloys, analyzed the effect of alloying with 3*d* and 5*d* transition metal elements on dislocation energetics, and established the electronic origins of the solid solution softening/hardening phenomena. We investigated the effect of topologically close packed phase formation on the solubility of interstitial impurities in Cr- and Mo-based alloys and demonstrated their effect in preventing the formation of embrittling phases. We showed that Co- and Y-based B2 intermetallics are intrinsically ductile, established the dislocation structure in Co-based alloys, analyzed the origins of their unusual mechanical behavior, and identified the microscopic origins of the yield stress anomaly.

15. SUBJECT TERMS

High temperature structural materials, intermetallic alloys, γ/γ' superalloys, large-scale modeling, electronic structure calculations, dislocation properties, brittle-ductile behavior, alloying, solid solution softening, yield stress anomaly

16. SECURITY CLASSIFICATION OF:			17. LIMITATION OF ABSTRACT	18. NUMBER OF PAGES	19a. NAME OF RESPONSIBLE PERSON
a. REPORT	b. ABSTRACT	c. THIS PAGE			Arthur J. Freeman
U	U	U	UU	22	19b. TELEPHONE NUMBER *(include area code)* (847)491-3343

Objectives

The objective of this research is to investigate the microscopic mechanisms governing the deformation and fracture behavior of ordered intermetallic aerospace alloys and metals in order to contribute to the development of a fundamental basis for computer-aided alloys design. The most important and challenging component of our research is to bridge the gap between a microscopic quantum-mechanical description of the chemical bonding and the mesoscopic phenomena which govern the mechanical response of intermetallics. The emphasis on the computational/simulation approach focuses on understanding "real" materials, which have an abundance of "defects" including impurities, dislocations or other faults, second phase precipitates, etc. - all of which are governed on the microscopic level by the electronic structure.

Research findings

1. Fundamental parameters of brittle-ductile behavior of platinum group metals alloys and prediction of cleavage-like crack propagation.

Ir- and Rh-based alloys attract considerable attention as promising materials for ultra-high-temperature applications. However, polycrystalline Ir, Rh and their alloys normally exhibit intergranular fracture with limited ductility in tensile tests up to elevated temperatures [1]. The lack of understanding of the fundamental characteristics which control brittle-ductile behavior in these alloys has hindered progress in this field.

The brittleness of Ir and Rh is intrinsic and is not caused by impurities at grain boundaries. As we showed in [2] the reasons for this behavior, which distinguishes Ir and Rh among other *fcc* metals, is connected with a "pseudo-covalent" character of the chemical bonding in these metals. As a result, the standard Rice-Thomson criterion for cleavage-like crack propagation [3] $\mu b/\gamma_s > 7.5 - 10$ is fulfilled for these metals due to relatively large elastic moduli in comparison with the decohesion energy.

In order to identify fundamental characteristics driving the fracture behavior of Ir- and Rh-based alloys, we performed *ab initio* calculations of decohesion energies and elastic moduli in Ir_3Nb, Ir_3Zr, Rh_3Nb, and Rh_3Zr alloys by means of the all-electron full-potential linearized augmented plane wave (FLAPW) method [4].

Table 1: Cauchy pressure $(C_{12}-C_{44})/C_{44}$, surface energy for {111} plane and Rice-Thomson ratio $\mu_{nb}b/\gamma_s$ for select refractory $L1_2$ alloys in comparison with Ni_3Al and ductile *fcc* metals.

Metal / alloy	$\frac{C_{12}-C_{44}}{C_{44}}$	$\mu_{nb}b$ (Gpa)	γ_s (J/m^2)	$\mu_{nb}b/\gamma_s$
Ni	0.15	68.5	2.3	7.6
Al	1.15	24.8	1.2	5.9
Ni_3Al	0.18	57.5	1.9	7.8
Ir	-0.05	198	2.5	24.5
Rh	-0.05	133	2.5	14.6
Ir_3Nb	-0.10	173	2.6	18.4
Ir_3Zr	-0.05	134	2.4	15.0
Rh_3Nb	-0.03	124	2.3	14.8
Rh_3Zr	0.11	87.6	2.0	12.2

The surface energy γ_s was determined from the asymptotic value of the ideal cleavage decohesion energy $E_{cl}^{max} = 2\gamma_s$, which required cleaving an infinite bulk crystal into two semi-infinite parts and the creation of two free

surfaces. One can see from Table 1, Ir- and Rh-based alloys (except for Rh_3Zr) as well as pure Ir and Rh, have negative Cauchy pressures, $(C_{12}-C_{44})/C_{44}$. This feature is in contrast with the Ni-based alloys and confirms the pseudo-covalent chemical bonding in Ir_3X and Rh_3X intermetallics. We found that in all the alloys considered, the minimal surface energy corresponds to the {111} plane. Though the shear modulus $\mu_{\mathbf{nb}}$ (where **n** is the normal to the {111} slip plane, **b** is shear direction ⟨110⟩) in refractory alloys was found to be 3 times larger than in Ni_3Al, the surface energy, γ_s, is only approximately 25% larger. As a result, the ratio $\mu_{\mathbf{nb}}b/\gamma_s$ for Ir- and Rh-based alloys exceeds significantly the Rice-Thompson critical value. Thus, based on the results of these calculations, we predict cleavage-like crack propagation in these alloys.

2. Superdislocation structure in Rh-based $L1_2$ alloys.

Two-phase γ/γ' nickel-based superalloys remain important structural materials for high-temperature applications. However, their potential for a further increase of the temperature capability of these materials has been exhausted. Recently, a new class of superalloys based on platinum group metals (PGM) with higher melting temperatures and superior environmental properties was proposed [5]. Among these, Pt-, Ir- and Rh-based alloys attract the most attention. Although Rh-based alloys have lower melting points compared to Ir alloys, they possess a large advantage in density. Moreover, it has been known that the oxidation resistance of Rh is superior to Ir [6]. Although there are few doubts as to the potential of the PGA for ultra-high temperature applications, further progress in their development is hindered due to an insufficient understanding of the fundamental factors that control their mechanical properties. In particular, there is no reliable information about dislocation structure and mobility in Ir and Rh-based alloys, except for a single observation of superdislocations in Ir_3Nb [7].

Recently, we used our theoretical combined *ab initio* and Peierls-Nabarro (PN) model approach to investigate the dislocation properties in Ir_3X alloys [8] and demonstrated that features of the dislocations in Ir-based alloys are closely connected with instability in relation to $L1_2 \rightarrow D0_{19}$ transformation. Now we focus on Rh group alloys and apply highly accurate first-principles calculations of the generalized stacking fault (GSF) energetics to relate the microscopic characteristic of interatomic interactions with properties of dislocation in Rh_3X intermetallics (where X = Ti, Zr, Hf, V, Nb, Ta).

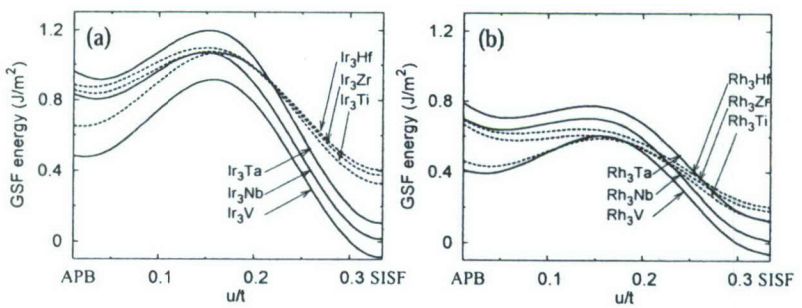

Figure 1: Section of the GSF surface in (a) Ir_3X and (b) Rh_3X alloys along ⟨112⟩ direction corresponding to the path from ideal APB to SISF positions.

In order to determine the GSF energies, $\Phi(\mathbf{u})$ which are associated with a rigid shift of one part of the crystal with respect to another on a fault vector **u** in the slip plane, we carried out total energy first-principles calculations using the all-electron FLAPW method [4] and a

supercell geometry with 6 atomic layers and homogeneous periodic boundary conditions. For Rh_3X we found a similar tendency as was observed earlier for Ir_3X intermetallics [8] (cf., Fig. 1). All alloys can be divided into two groups: Rh alloys with IVA elements (Hf, Zr, Ti) which have a "normal" ratio of the superlattice intrinsic stacking fault (SISF), γ, to antiphase boundary (APB) energy ζ_{111} and alloys with VA elements (Ta, Nb, V) which have a small γ/ζ_{111} ratio. The decrease of the SISF energy by replacing of IVA alloying elements with VA has an electronic origin [8] and is a common feature of both Ir- and Rh-based alloys.

For analyses of the dislocation properties, we employ our combined approach based on *ab initio* γ-surface energetics and larger scale modeling within the PN model. The dislocation structure is shown in Fig. 2 as a "splitting path" together with the γ-surface for Rh_3Ta, Rh_3Zr and Rh_3Nb. We found that superdislocations with type II core structure (Kear splitting scheme with the SISF ribbon between partials) are strongly preferred energetically in Rh_3Nb (Fig. 2(c)), and type I superdislocations (with APB ribbon between partials) are predicted for Rh_3Ta (Fig. 2(a)) and Rh_3Ti.

The Rh_3X intermetallics are distinguished from Ir_3X by a relatively small value of the energy barrier between APB and SISF (Fig. 1); the barrier practically disappears for Rh_3Hf and Rh_3Zr. As a result, an unusual superdislocation core structure was found in Rh_3Hf and Rh_3Zr (Fig. 2(b)). Because of the very shallow APB minima, type I dislocations become unstable, and SISF bounded type II' (with different sequence of Shockley partials [9]) is preferable.

Thus, among the Rh_3X intermetallics we predict that type I dislocations will be present only in Rh_3Ti and Rh_3Ta, and type II superdislocations in other cases. There are two reasons for the appearance of SISF bounded superdislocations: (i) a low γ/ζ_{111} ratio, and (ii) an unstable APB energy; these conditions result in the appearance of type II and type II' superdislocations, respectively.

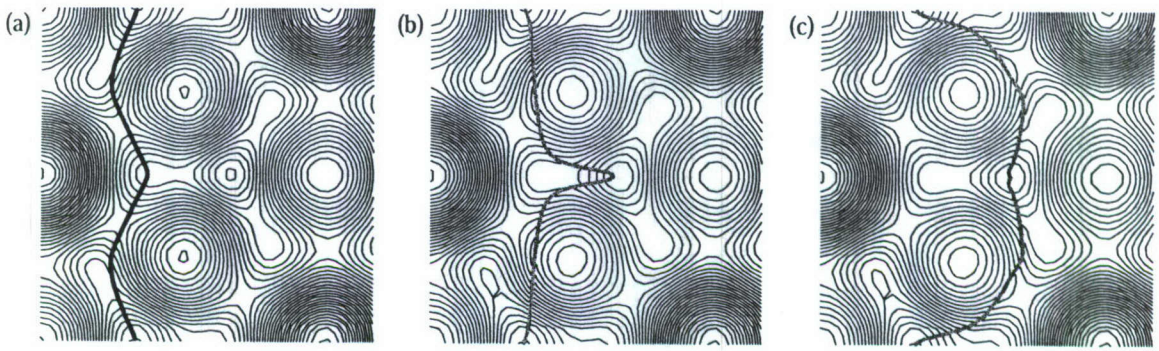

Figure 2: Contour plots of the generalized stacking fault energies for $L1_2$ (a) Rh_3Ta, (b) Rh_3Zr and (c) Rh_3Nb; the structures of the superdislocations are shown as "splitting paths" (bold curves).

3. Temperature dependence of the lattice misfit in γ/γ' superalloys. Role of thermal expansion and composition changes.

The magnitude of the lattice misfit between the γ and γ' phases, $\delta = 2(a_{\gamma'} - a_{\gamma})/(a_{\gamma'} + a_{\gamma})$ (where a_{γ}, $a_{\gamma'}$ are the lattice constants for the corresponding phases), is one of the key parameters which determines the microstructure formation, stability and mechanical behavior

of modern high-temperature superalloys. To attain a stable alloy microstructure ensuring the high creep and thermal resistance, the misfit parameter should have an optimal value at the operational temperature.

Experimentally, the dependence $\delta(T)$ in the Ni-based alloys exhibits a slight decrease in the temperature range up to 900°C and a rapid fall for $T > 900$°C [10]. In Ir-based alloys, the $\delta(T)$ shows a very small variation in the temperature region up to 1500°C [11].

The relative importance of two contributions to the temperature dependence of $\delta(T)$ are under intense investigation, namely: (i) the difference in thermal expansion of the two phases [12], and (ii) the redistribution of alloying component between γ and γ' with the increase of temperature [13].

We explore the role both thermal expansion and composition changes in $\delta(T)$ for the Ni-Al and Ir-Nb γ/γ' two-phase alloys based on *ab initio* total energy and phonon spectra calculations. The thermal expansion and lattice misfit were calculated in the framework of the quasi-harmonic approximation on the basis of the linear response theory for phonon spectra in Ni, Ir, Ni_3Al, Ir_3Nb using the pseudopotential method [14]. High precision calculations of the lattice parameter changes due to Al(Nb) substitutions in the Ni(Ir) matrix and antisite defects in the γ' phase were performed on the basis of total energy calculations using the highly accurate FLAPW method [4].

The results of calculations of the thermal expansion coefficients, $\alpha(T)$, and the temperature dependence of the bulk moduli, $B(T)$, for Ni, Ni_3Al, Ir, I_3Nb (Fig. 3) are in good agreement with available experimental data. A small deviation from experiment for Ni and Ni_3Al indicates that the quasi-harmonic approximation becomes less accurate at high temperatures. Our results also clearly demonstrate the important contribution of the ferromagnetism of Ni to its $B(T)$ behavior.

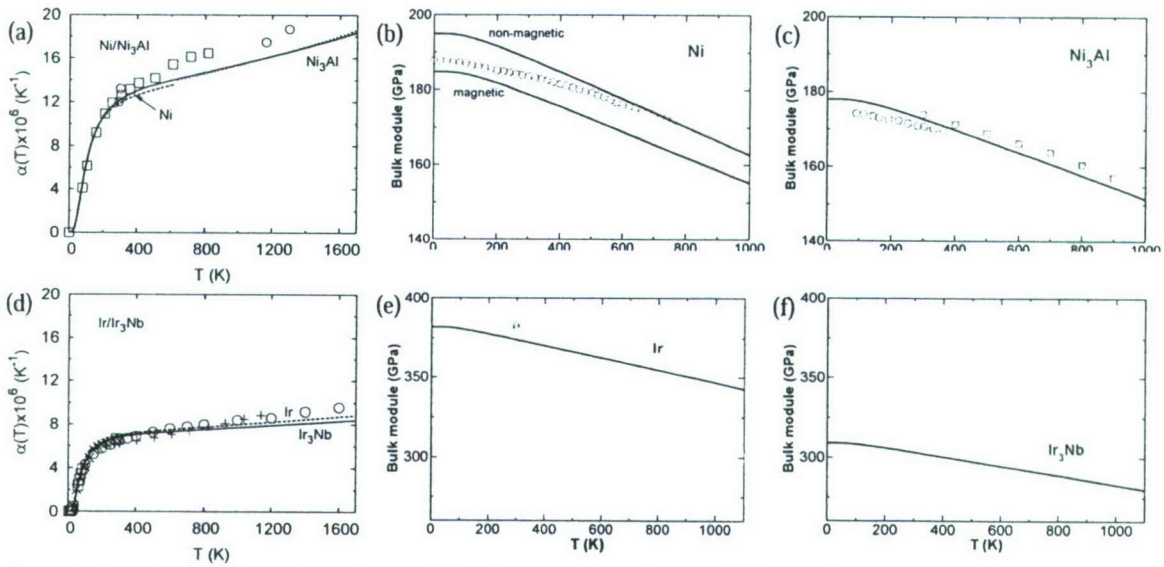

Figure 3: The temperature dependence of the thermal expansion coefficient $\alpha(T)$ (a,d) and bulk moduli $B(T)$ (b,c,e,f) for Ni/Ni_3Al (a-c), Ir/Ir_3Nb (d-f). The symbols mark the experimental data.

Since the values of the thermal expansion coefficients $\alpha(T)$ are very similar between the γ and corresponding γ' phases (Fig. 3(a),(d)), the thermal expansion results in a very slow variation of the lattice misfit $\delta(T)$ with temperature (Fig. 4(a),(b)). Such behavior is in agreement with experiment for Ir/Ir_3Nb (Fig. 4(b)), but drastically different from the observed $\delta(T)$ dependence for the Ni/Ni_3Al alloys (Fig. 4(a)). The latter indicates that the redistribution of alloying elements between phases could be the main contributor to the lattice misfit dependence at high temperatures. The concentration dependence of the lattice parameters can be presented in the form:

$$a_\gamma(c) = a_\gamma^{(0)}(1 + c_\gamma \beta_\gamma), \qquad a_{\gamma'}(c) = a_{\gamma'}^{(0)}(1 + (c_{\gamma'} - 0.25)\beta_{\gamma'}),$$

where c_γ, $c_{\gamma'}$ are concentrations of the redistributed component, and β_γ, $\beta_{\gamma'}$ are the concentration expansion coefficients, da/dc, in the γ and γ' phases, respectively. The values of β were obtained from FLAPW calculations of the volume changes of 32-atom supercells with 3.125% of the redistributed component, and are as follows: β_γ=0.059, $\beta_{\gamma'}$=0.049 for Ni/Ni_3Al and β_γ=0.062, $\beta_{\gamma'}$=0.04 for Ir/Ir_3Nb. The temperature dependence of the concentrations $c_\gamma(T)$, $c_{\gamma'}(T)$ were assumed to follow the solubility lines in the γ and γ' phases on the phase diagram (curves 1, 2 in Fig. 4(c),(d)); this is true for two-phase systems in thermal equilibrium. The calculated effect of the composition changes is presented in Fig. 4(a). It is seen that its slope is very close to the experimental values at high temperatures. At low temperatures (< 600 K) where the thermal diffusion is suppressed, the lattice misfit follows the behavior predicted from the thermal expansion alone, i.e. it increases slightly.

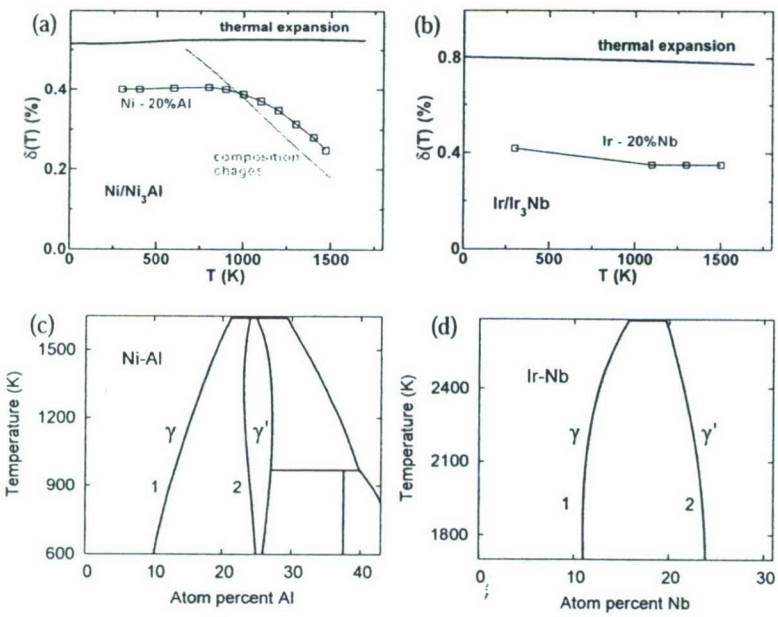

Figure 4: Contributions of the thermal expansion and composition changes to the temperature dependence of the constrained lattice misfit $\delta_c(T) = \delta(T) \cdot 3B/(3B+4\mu)$ for (a) Ni/Ni_3Al and (b) Ir/Ir_3Nb (μ is the shear modulus). Rectangles correspond to the experimental data; (c) Ni-rich and (d) Ir-rich parts of equilibrium phase diagrams for Ni-Al and Ir-Nb alloys, respectively.

Thus, the redistribution of the major alloy components (Al into Ni and Ni into Ni_3Al) gives the main contribution to the temperature dependence of the lattice misfit and the behavior of $\delta(T)$ for Ni/Ni_3Al at high temperatures. For the Ir/Ir_3Nb system, the alloy component redistribution will start to contribute to the lattice misfit only at extremely high temperatures (>2000 K). The amplitude of these contributions can be determined by considering the shape of the γ - γ' gap on phase diagrams. The last conclusion is important for alloy design as it allows one to establish a simple relation between the alloy phase diagram and the temperature dependence $\delta(T)$.

4. The electronic origin of solid solution softening in bcc molybdenum alloys.

The addition of elements which improve the room temperature strength and high temperature creep resistance of materials, is important in alloy design. Besides the solid solution hardening effect (SSH), which is connected with the pinning action of impurities on dislocations, in some cases the alloying can lead to the opposite phenomenon, the decrease of hardness, which is known as solid solution softening (SSS). The SSS effect is well studied in *bcc* transition metal alloys and attracts remarkable attention as a possible way to improve the low temperature ductility of the refractory group VIA *bcc* metals (Cr, Mo, W) [15].

It is commonly accepted, that the intrinsic solution softening is connected with direct impurity-dislocation interactions and results from the enhanced kink nucleation at point defects [16]. However, the microscopic mechanism of this phenomenon still remains a matter of discussion. In particular, the changes in hardening rate, *dH/dc*, for Mo alloys correlate with atomic size misfit only for W, Ta, Hf leading to SSH and not for Pt, Ir, Os, Re, which promote softening for low solute concentration and low temperatures [15],[17]. Moreover, for binary and ternary Mo alloys there is a strong correlation between softening rates and the number of extra electrons brought by solute elements [17]. These results clearly indicate the importance of the "chemical" mechanism of impurity-dislocation interactions in the SSS.

Here we present an investigation of the microscopic mechanisms of SSS in binary Mo alloys on the basis of *ab initio* electronic structure calculations. Our calculations are inspired by the observation that SSS results from the addition of certain alloying elements which decrease the stacking fault energy (SFE) [18] - one of the key parameters which control the dislocation structure. We calculated the GSF energies in molybdenum alloying with 5*d* and 3*d* transition metal elements and showed that the SSS in Mo alloys can be explained by the decrease of the energy barrier for kink nucleation due to the local lowering the SFE at the substitutional atoms. The total energy calculations were carried out by the first-principles full-potential linear muffin-tin orbital (FLMTO) method [19].

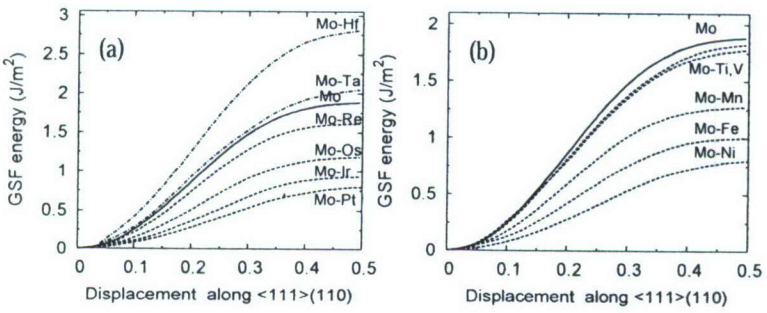

Figure 5: GSF energies for ⟨111⟩{110} shear in Mo and Mo alloys with (a) 5*d* and (b) 3*d* elements. The *x* axes are given in units of the Burgers vector 1/2⟨111⟩.

The GSF energies estimated for (100) planar shifts along ⟨111⟩ (parallel to the Burgers vector) are shown in Fig. 5 for *bcc* Mo and Mo alloys. All 5*d* TM additions with an extra electron concentration lead to the reduction of the GSF energy in comparison with unalloyed molybdenum. The energy of the unstable stacking fault, γ_{us} (corresponding to the maximum of the GSF energy in Fig. 5), decreases monotonically with the atomic number of the solute atoms (cf. Table 2). The additions that reduce the electron concentration (Ta, Hf) as well as an isoelectonic impurity (W) lead to an increase in the GSF

Table 2: The ratio of stacking fault energies $\gamma_{us}/\gamma^0_{us}$ (γ^0_{us} corresponds to unalloyed Mo), the ratio of the t_{2g}/e_g occupations for addition atoms, the ratio of ionic radii R_i/R_{Mo} and initial hardening rate [5], dH/dc, for binary molybdenum alloys.

	Hf	Ta	W	Re	Os	Ir	Pt
$\gamma_{us}/\gamma^0_{us}$	1.49	1.09	1.02	0.86	0.63	0.46	0.38
t_{2g}/e_g	1.86	1.85	1.86	1.81	1.73	1.58	1.41
R_i/R_{Mo}	1.13	1.05	1.01	0.99	0.96	0.97	0.99
$dH/dc \cdot 10^2$	10	5	~0	-5	-35	-70	-120

energy and the additions with excess electrons (Re, Os, Ir and Pt) lower its value. The decrease in GSF energy obtained in the row of solutes from Re to Pt strongly correlates with the experimentally observed lowering of the initial hardening rate [17] (i.e. dH/dc for C approaching zero) at 77 K (Table 1). Thus, the calculated results point out that the SSS mechanism in Mo alloys should be connected with the decrease in GSF energy, similar to that established in [18] for *fcc*-based alloys. Similar trends were obtained for 3*d* TM solutes, but in this case all elements including Ti and V lead to a decrease of γ_{us}. Hence, based on these results one can also predict the SSS effect for 3*d* solutes with extra electrons.

To make clear the relation between the chemical bonding and the GSF energy characterizing the lattice resistance to $\langle 111 \rangle (110)$ shear deformation, we analyzed the changes in the orbital occupations for additions in Mo binary alloys. For the *bcc* structure, the t_{2g} and e_g orbitals are responsible for the directional bonds between the nearest neighbor atoms (*nn*, along the $\langle 111 \rangle$ direction) and second (next nearest) neighbors (*nnn*, along $\langle 100 \rangle$), respectively. We found that the local changes in the occupation anisotropy correlate with the GSF energy (cf., Table 1) and point out that the decrease in the shear resistance is connected with the weakening of the *nn* bonds relative to *nnn* near the solute atom.

Thus, the calculated trends in the GSF energies confirm the suppositions based on the experimental investigations [17] concerning the electronic nature of the SSS. This conclusion is not trivial because there is no simple relation between the GSF energy and kink formation in *bcc* metals. As established in recent calculations (see [20] and references therein), the screw dislocation in Mo has a nondegenerate core, spread symmetrically into the three (110) planes. We suggest that a solute atom locally disturbs the three-fold symmetry of the dislocation core due to the lowering of the GSF energy for one of the three (110) planes. The barrier for double kink nucleation can be roughly estimated from the energy difference $\Delta E_{2\text{-}3}$ between a plane core with a solute atom and the three-fold core in the matrix [21],

$$\Delta E_{2-3} = \frac{\mu b^2}{4\pi} \ln\left(\frac{1.2\gamma_{us}}{\gamma^0_{us}}\right).$$

Both 3*d* and 5*d* transition metals lead to a monotonous decrease in $\Delta E_{2\text{-}3}$ and the energy barrier for double kink nucleation with atomic number for additions with extra electrons. Thus, we demonstrated that the tendencies in SSS can be understood in terms of the effect of solute atoms on the GSF energy.

5. Effect of additions on dislocation structure and mobility in bcc Mo. Atomic row model with ab initio parameterization.

A strong correlation between the softening behavior, unstable stacking fault energy and number of valence electrons introduced by alloying additions in bcc Mo alloys discussed above clearly points out an electronic origin of the solid solution softening and emphasizes the importance of the changes in dislocation structure due to solutes.

In bcc metals, plastic deformation is realized by the motion of screw dislocations with a star-like nonplanar core, and being a planar defect the stacking fault does not characterize the dislocation structure quite accurately. To investigate the effect of additions on the core structure, we employ a combined approach that includes the atomic row model for a screw dislocation in bcc metals [22] with *ab initio* parametrization of the interatomic row potentials, $\Phi(u)$. The potential $\Phi(u)$ is assumed to be a function only of the relative atomic positions, u, and is composed of the first and second terms in the Fourier expansion:

$$\Phi(u) = \frac{\Phi_0}{(1-4\alpha)}\left(\cos\frac{2\pi u}{b} - \alpha\cos\frac{4\pi u}{b} + \frac{1}{2}(1-\alpha)\right), \quad (1)$$

where b is the Burgers vector. The energy variation under the atomic row shift along $\langle 111\rangle$,

$$\Delta E_{row}(u) = 3(\Phi(u-1/3) + \Phi(u+1/3)), \quad (2)$$

was calculated using the first-principles full-potential linear muffin-tin orbital (FLMTO) method [19] and the parameters Φ_0 and α found from Eqs. (1) and (2). The dislocation core structure is determined by the relaxation of each atomic row position, u_i, with appropriate boundary conditions to its equilibrium value to provide a minimum of the total energy.

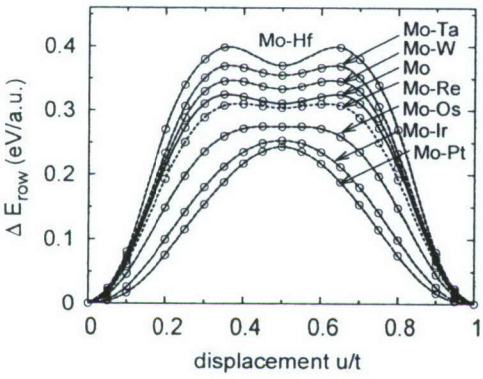

Figure 6: Atomic row displacement energies, ΔE_{row}, for a shift of the atomic row with solute along $\langle 111\rangle$ versus displacement in units of the Burgers vector $1/2\langle 111\rangle$.

The calculated atomic row displacement (ARD) energy, ΔE_{line}, (Fig. 6) decreases for the solutes with extra electrons (Re, Os, Ir, Pt) and increases for additions that reduce the electron concentration (Hf, Ta and W). The changes in atomic row shift resistance correlate with the variation of γ_{us} [23] and with the observable trend in SSS [24]. The effect of additions is not localized in the atomic row with the solute, but covers the region of the nearest atoms around the solutes.

We demonstrated that the atomic row model with *ab initio* parametrization of the interatomic row potential gives the correct description of the dislocation structure. In particular, we found a compact isotropic core structure in Mo that is in agreement with the results of direct first principles calculations [25]. We modeled the effect of the solute by the relevant change in the interatomic row potential and found that the solute in the "easy" dislocation core disturbs the three-fold symmetry due to (i) local distortions in Re and Os or (ii) a transformation to the split (Fig. 7a,b) or spread (Fig. 7c) core structure for Ir and Pt additions. The softener additions (with extra electrons) attract the dislocation in

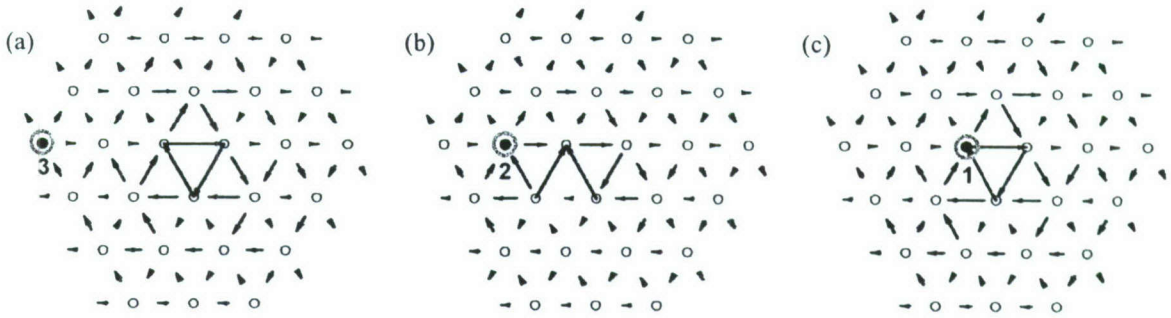

Figure 7: Effect of Pt additions (shown by filled circle) on the "easy" dislocation core structure: (a) slightly distorted core due to Pt in position 3 far from the dislocation core, (b) split core structure due to solute in position 2, (c) spread core structure with solute in the dislocation core (position 1).

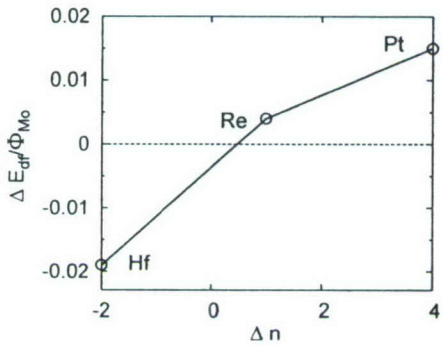

Figure 8: The contribution to the driving force for double kink nucleation, ΔE_{df}, for Pt, Re, and Hf additions.

contrast with hardeners which have repulsive solute–dislocation interactions. As a result, softener additions will promote double kink nucleation because they produce an extra driving force (Fig. 8) for bowing the dislocation line.

Thus, the atomic row model predicts, in agreement with experiment, the enhancement of double kink nucleation due to softener solutes. Because ARD energies gradually change with the band filling in alloys for softener additions, our findings allow one to explain the observed correlation between SSS and the atomic number of the solute [24].

6. Solid solution softening and hardening in the Group V and Group VI refractory bcc transition metal alloys. Atomic row model with ab initio parameterization.

In contrast with the Group VIA alloys, the softening in the Group VA (V, Nb, Ta) bcc metal alloys was traditionally considered as an extrinsic phenomenon originating from the scavenging of interstitial impurities by the solutes [26]. Recently, however, the Peierls mechanism was suggested as responsible for hardening rates in Ta-W alloys at low temperatures [27],[28]. As result, the question about the microscopic mechanism for the hardening/softening behavior in the Group VA bcc refractory metals is still open to discussion. Here we present the results of comparative investigations of the solution softening in the Groups VA (Nb, Ta) and VIA (Mo, W) metal alloys. Direct investigations of the solute–dislocation interaction by first principles electronic structure calculations are still a difficult problem. To make clear the effect of additions on the dislocation core structure and mobility, we employ our combined approach [23],[29], which includes the atomic row model (ARM) for a screw dislocation in bcc metals with the atomic row displacement energy, ΔE_{row}, calculated using the *ab initio* full-potential linear muffin-tin orbital (FLMTO) method [19].

The dependence of $\Delta E_{row}(u)$ on the relative atomic row displacement u is shown in Fig. 9.

The value of ΔE_{row} decreases gradually with the number of extra valence electrons of solutes (Re, Os, Ir, Pt) in both Mo and W (Fig. 9(a,b)) and these trends correlate with the experimental initial hardening rates. For the Group VA metals, we obtained the opposite result: the $4d$, $5d$ additions with extra valence electrons increase the atomic row shift resistance and the additions with a lack of electrons reduce $\Delta E_{row}(u)$. This difference originates from the peculiarities of the electronic structure and chemical bonding, when the Fermi level is located in the region of the bonding states (Group VA) or in the pseudogap between bonding and antibonding states (Group VIA).

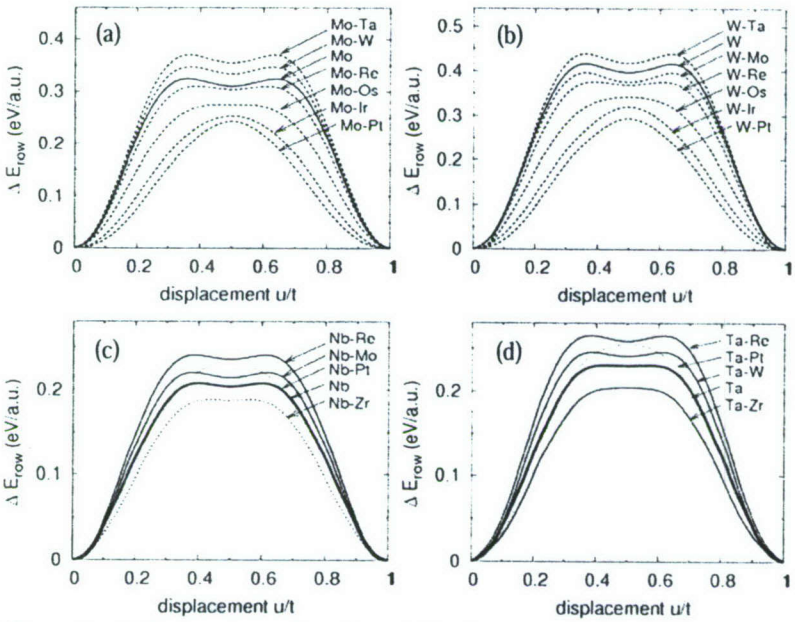

Figure 9: ARD energies, ΔE_{row}, for a shift of atomic row with solute along $\langle 100 \rangle$ in (a) Mo, (b) W, (c) Nb and (d) Ta alloys.

Using the atomic row model with *ab initio* parameterization, we found that the screw dislocations in pure Mo, W as well as in Nb and Ta metals have isotropic compact cores. The driving forces for the double kink nucleation – determined as total energy changes when a dislocation moves from a far position to the solute – are presented in Fig. 10. The softener additions which decrease the ARD energy have an attractive interaction with the dislocation, in contrast with alloying elements that increase $\Delta E_{row}(u)$ and have a repulsive interaction with dislocations. For the Group VA alloys, the effect of solutes on the driving forces is weaker and does not demonstrate the monotonic dependence on the number of valence electrons (Fig. 10). The additions with extra electrons in the Group VIA metals enhance the double kink nucleation and result in softening, but they lead to a repulsive interaction with dislocations and cannot be intrinsic softeners in the Nb and Ta alloys. By contrast, the solutes that lack electrons suppress the kink formation in the Group VIA metals, and promote it in the Group VA metals. In agreement with experiment [30], a strong strengthening effect in Nb and Ta was found for the Re additions,

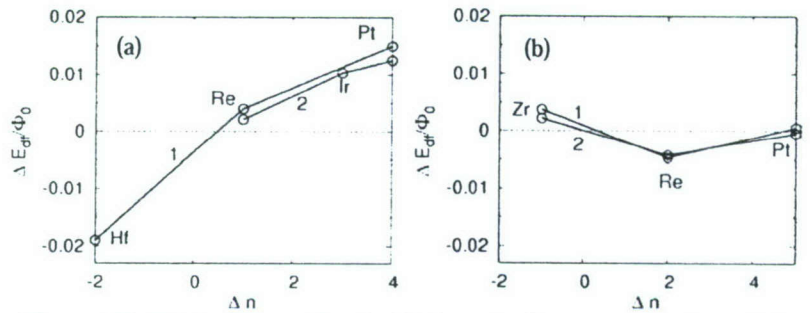

Figure 10: Driving force for the kink nucleation as a function of the difference in the number of valence electrons for (a) the Group VIA alloys (1 - Mo, 2 - W) and (b) Group VA alloys (1 - Nb, 2 - Mo).

in contrast with the Group VIA alloys where Re results in softening [15].
Thus, our results allow one to conclude that the effect of alloying with 4*d* and 5*d* transition elements on dislocation structure and mobility is fundamentally different for the bcc refractory metals of Groups VIA and VA. The additions with extra valence electrons, which give rise to SSS in the Group VIA metals, cannot lead to intrinsic softening in the Group VA metals. Oppositely, the additions with a lack of electrons (leading to strong hardening in Group VI metals) may result in intrinsic softening in the Group V metals, which is controlled by the double kink nucleation mechanism. We believe that the softening observed in Group V metals alloyed with Mo, W, and Re is governed instead by the extrinsic mechanisms – for example, by scavenging of solute interstitials. For the first time, we demonstrated that both softening and hardening effects in the bcc refractory metals are determined by the electronic structure rather than by atomic size or shear modulus misfits which are traditionally considered as the main parameters controlling the hardening/softening.

7. Electronic mechanism of the stabilization of A15 phase in Cr and Mo alloys by light impurities.

Alloys based on the group VI-A refractory bcc metals (Cr, Mo, W) are attractive materials for high-temperature applications. Among them, chromium alloys have advantages due to low density, high creep and oxidation resistance [31], and molybdenum alloys attract special attention due to their potential for aerospace applications. Unfortunately, the lack of ductility at low temperatures has severely limited the use of bcc refractory metals, whose room temperature brittleness is caused by extrinsic factors – extremely low solubility of interstitial impurities (C, N, O) resulting in the formation of brittle carbides, nitrides and oxides.

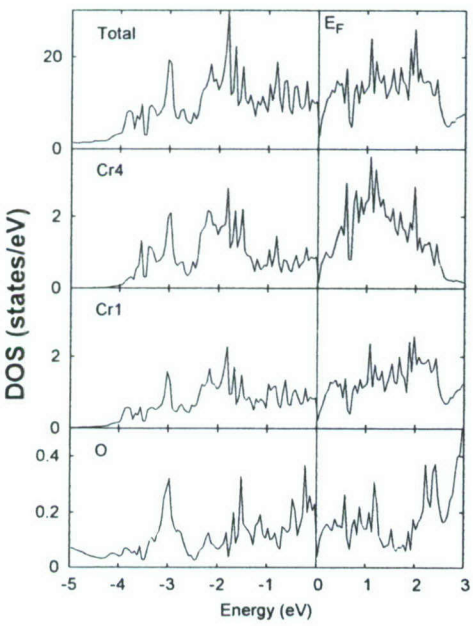

Figure 11: Electronic densities of states for A15 Cr with interstitial O.

Our recent *ab initio* calculations [32] showed that small Cr-Re clusters with TCP A15 structure may become energetically favored by the trapping of carbon impurities. This finding supports a proposed mechanism [33] of the "rhenium ductilizing effect" which connects the increase of the solubility of impurities with the appearance of TCP particles. These particles serve as efficient "attractors" of interstitials and prevent the formation of brittle phases and grain boundary segregation.

Further, we evaluated the role of light impurities (O, N, C) on the stabilization of the A15 phases of Cr and Mo on the basis of first-principles FLAPW [4] calculations. The A15 phases of pure Cr and Mo are metastable, higher in energy than the bcc phase by only 70 and 84 meV/atom for Cr and Mo, respectively. For the A15 Cr and Mo phases with oxygen impurities, both substitutional and interstitial positions were investigated. In all cases, full atomic relaxations were performed, and lowest energy

configurations were obtained. Substitutional structures were found to be very unstable, while the formation of the interstitial A15-O phase is energetically favored. As seen from Fig. 11, the stabilizing effect of interstitial oxygen in A15 Cr is a result of strong hybridization of O2*p* and Cr3*d* states over the whole bonding energy range, which also manifests itself by the opening of a sharp and deep DOS minimum exactly at the Fermi energy. For the A15 Mo phase, a similarly strong hybridization of O2*p* and Mo4*d* states takes place.

Table 3: Lattice parameters of A15 Cr and Mo phases with interstitial impurities and their stability with respect to bcc Cr(Mo) with interstitial impurities.

Structure	*a* (Å)	*c/a*	*E*(A15)-*E*(bcc) (eV/atom)
A15Cr+O_{int}	4.593	1.058	0.05
A15Cr+N_{int}	4.571	1.063	0.14
A15Cr+C_{int}	4.551	1.080	0.13
A15Mo+O_{int}	5.069	1.038	0.08
A15Mo+N_{int}	5.058	1.039	0.17
A15Mo+C_{int}	5.054	1.045	0.20

The formation energies were calculated for A15-type structures with O, N and C interstitials. Table 3 presents calculated lattice parameters and tetragonality of the structures; these compare favorably with available experiments on metastable A15 phases observed in thin films [34]. In bulk Cr, these structures will compete with interstitials in the bcc phase. The calculated energy difference, ÄE = E(A15) – E(bcc) (Table 3), shows that the configurations with interstitials in the bcc phase are still more energetically favored than in the A15 phase, and oxygen interstitials are the most preferred for the formation of the A15 phase. Thus, A15 Cr and Mo are impurity-locked metastable phases.

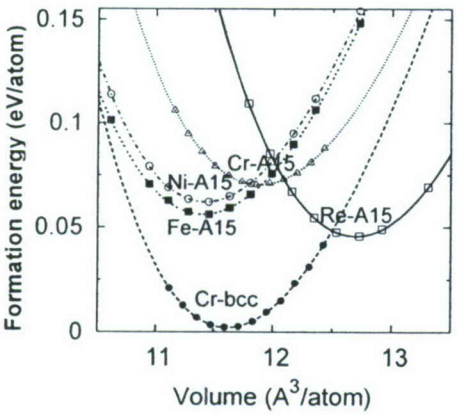

Figure 12: Formation energy for A15 Cr_3M phases in comparison with bcc and A15 Cr.

The effect of alloying Cr and Mo as a means to facilitate the formation of the A15 phase was then investigated. The following alloying elements were chosen for Cr alloying: Re, a known ductilizer, and Fe and Ni, which were conceived as possible Re alternatives. The calculated formation energies for Cr_3M (M = Re, Fe, Ni) compounds in the A15 structure, shown in Fig. 12 as a dependence of the formation energy on the volume, indicate that, while these phases remain metastable, they have lower energy compared to the A15 phase of Cr, with Cr_3Re showing the largest energy decrease. For Mo, only the effect of alloying with Re was investigated. The calculations of Mo_3Re in the A15 structure indicate that, similarly to Cr, it has lower formation energy (+0.052 eV/atom) compared to the A15 phase of Mo (+0.084 eV/atom). Thus, the alloying with Re increases the stability of the A15 phase of Mo.

The cumulative effect of both alloying and interstitial oxygen was investigated further. In addition to the formation energies, the energy gain resulting from oxygen interstitials was also calculated as: $E_{gain} = E_{tot}(Cr(Mo)_3M) + ½E_{tot}(O_2) - E_{tot}(Cr(Mo)_3M+O_{int})$. As seen from Table 4, the energy gain is highest for Cr_3Re and Mo_3Re, where it is 2 and 6 times higher

Table 4: Energy gain due to O interstitials and formation energy of A15 $Cr(Mo)_3M+O_{int}$.

System	E_{form} (eV/atom)	E_{gain} (eV/oxygen)
Cr_3Fe+O_{int}	+0.023	0.24
Cr_3Ni+O_{int}	-0.026	0.71
Cr_3Re+O_{int}	-0.127	1.38
Mo_3Re+O_{int}	-0.143	1.56

than for Cr_3Ni and Cr_3Fe; respectively. This is a result of both strong O-Re bonding and lattice expansion due to Re alloying; the latter creates a larger interstitial pore that accommodates the oxygen atom better leading to a smaller structural deformation. As a result, the formation energy for A15 Cr_3Re and Mo_3Re with O interstitials becomes largely negative, confirming the stability of these structures.

Finally, the formation energy for the $Cr(Mo)_3Re+O_{int}$ phase was compared with that of the O interstitial in the bcc Cr(Mo)-25% Re alloy, and the preference energies $E_{pref} = E_{tot}$(A15 $Cr(Mo)_3Re+O_{int}$) – E_{tot}(bcc Cr(Mo)-25%$Re+O_{int}$) were calculated. The preference energies of -0.064 eV/atom and -0.057 eV/atom were obtained for Cr_3Re+O_{int} and Mo_3Re+O_{int}, respectively. Thus, based on precise first-principles total energy calculations, we demonstrate that Re alloying in the presence of light elements may result in the formation of stable $Cr(Mo)_3Re$+interstitial precipitate particles with A15-like structure. These particles can act as scavengers of light impurities, increase impurity solubility and thus directly improve the ductility of Mo alloys.

8. Fundamental parameters of the brittle–ductile behavior of B2 intermetallics.

The transition metal (TM) aluminides, NiAl, CoAl, and FeAl, attract considerable attention as potential structural materials due to high strength, environmental resistance and low density; however, they show brittleness at ambient temperatures. The low ductility of TM aluminides comes from intrinsic reasons and is connected with their susceptibility to cleavage-like crack propagation [35] and an insufficient number of slip systems. Recently, a whole new class of ductile B2-type intermetallics compounds, based on rare-earth elements (such as YCu, YAg, and YZn) has been discovered [36]. In addition, high ductility was found in CoZr [37], which belongs to a unique group of Co-based B2 CoX intermetallics (X = Ti, Zr, Hf) exhibiting a positive temperature dependence of the yield stress [38].

Table 5: Elastic modulus C_{44}, ratio of C_{44} to bulk modulus B, surface energy for {110} plane γ_s, and Rice-Thomson ratio $\mu b/\gamma_s$ for TM aluminide, Co- and Y-based B2 intermetallics.

Alloy	C_{44} (GPa)	C_{44}/B	γ_s (J/m^2)	$\mu b/\gamma_s$
NiAl	153	0.85	1.64	27.6
CoAl	145	0.81	2.23	18.8
FeAl	120	0.76	2.39	14.4
CoTi	63	0.35	2.00	9.4
CoZr	43	0.28	1.77	7.6
CoHf	56	0.35	1.89	9.3
YCu	33	0.49	1.15	10.5
YAg	34	0.52	1.01	12.2
YZn	40	0.69	1.05	14.3

To identify fundamental characteristics driving the fracture behavior of B2 intermetallics, we calculated the decohesion energies and elastic moduli in TM aluminides and Co- and Y-based alloys (Table 5) by means of first-principles total energy FLAPW [4] calculations. The surface energy, γ_s, was determined from the asymptotic value of the ideal cleavage decohesion energy $E_{cl}^{max} = 2\gamma_s$ required to cleave an infinite bulk crystal into two

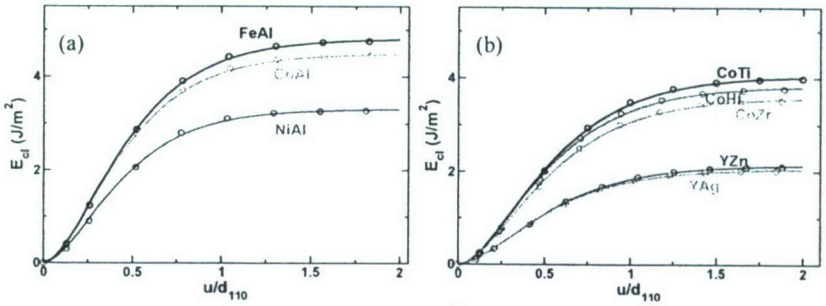

Figure 13: Decohesion energy, E_{cl} (J/m^2), as a function of the separation distance u (in units of the {110} interplane distance d_{110}) in (a) TM aluminides and (b) Co- and Y- based alloys.

semi-infinite parts and the creation of two free surfaces (see Fig. 13).

It is seen from Table 5 that Co- and Y-based alloys are distinct from TM aluminides by the low C_{44} shear modulus. The small C_{44}/B ratio indicates possible lattice instability with respect to martensitic transformation. Indeed, YCu and CoTi alloys were found to undergo at low temperatures the B2→B27 and B2→B19 transformation, respectively. According to the Rice-Thomson criterion [3], cleavage-like (brittle) crack propagation is expected if the condition $\mu b/\gamma_s > 7.5$-10 is fulfilled. (Here, b is the Burgers vector, μ the shear modulus; $\mu = C_{44}$ for ⟨100⟩{110} shear). Even though the shear moduli of Co- and Y-based alloys are 3-5 times lower compared to TM aluminides, the difference in the surface energy γ_s is much less. As a result, the ratio $\mu b/\gamma_s$ is significantly higher for TM aluminides and exceeds the Rice-Thompson's critical value resulting in cleavage-like crack propagation. At the same time, we predict ductile behavior for Co-based alloys and YCu and YAg, due to the plastic relaxation processes in a crack tip, and low fracture toughness for YZn; these findings agree with experiment. Thus, the observed ductility of Co- and Y-based B2 intermetallics has intrinsic origins and is connected with the low shear resistance combined with the relatively high decohesion energy.

9. Dislocation structure and mobility in B2 CoZr: combined ab initio-Peierls-Nabarro analysis.

As mentioned above, Co-based intermetallics satisfy the Rice-Thomson criteria for ductile behavior, and remarkable plasticity was observed recently in CoZr [37]. In addition, these alloys are unique among B2 intermetallics due to a positive yield stress dependence on temperature [38], despite the fact that only ⟨100⟩ dislocations operate in plastic deformation. To understand the origin of the unusual mechanical behavior of Co-based alloys, an investigation of the dislocation properties is necessary. Experimentally, there is only one HREM observation of dislocations in CoTi [39].

Table 6: Relaxed unstable stacking fault energy γ_{us}^{relax} for ⟨100⟩{011} shear, ratio $\gamma_s/\gamma_{us}^{relax}$ and width of dislocation core d, for CoZr and NiAl.

Alloy	γ_{us}^{relax} (J/m^2)	$\gamma_s/\gamma_{us}^{relax}$	d/a
CoZr	0.19	9.8	6.6
NiAl	1.36	1.2	2.4

To investigate the structure and mobility of ⟨100⟩ dislocations in B2 Co-based intermetallics, we employ our approach which combines the modified Peierls-Nabarro model with *ab initio* generalized stacking fault (GSF) energetics. We found that GSF energies for {001} and {110} planes in CoZr are significantly smaller compared with NiAl, and the lowest shear resistance corresponds to the {110} slip plane

(previously, we reported similar behavior for CoTi). Most striking is a dramatic decrease of the GSF energy for ⟨100⟩{011} shear due to atomic relaxation in CoZr, in contrast with NiAl where the GSF energy remains high after relaxation (Fig. 14). In particular, the unstable stacking fault energy, γ_{us}, decreases from 1.07 to 0.18 J/m^2 in CoZr for the {110} plane and from 1.95 to 0.87 J/m^2 for the {001} plane. This results in a high value of the γ_s/γ_{us} ratio (see Table 6) that indicates ductile behavior of CoZr according to a criterion proposed in [40].

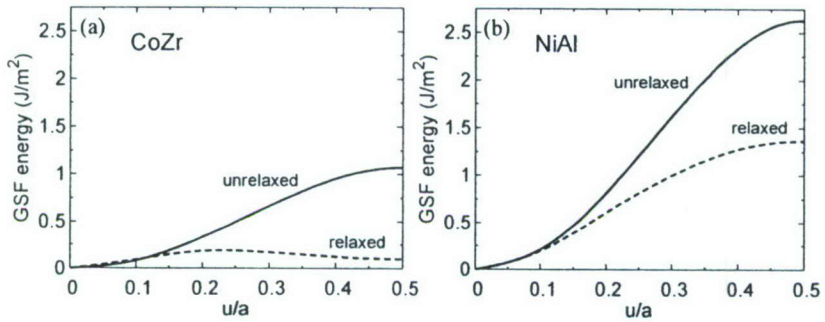

Figure 14: ⟨100⟩{011} section of the ã-surface in (a) CoZr and (b) NiAl before and after atomic relaxation perpendicular to the slip plane direction.

Taking unto account the GSF relaxation, we predict the splitting of the ⟨100⟩{011} dislocation structure in CoZr to occur according to the following scheme: **b** = **b**/2 + **b**/2 (Fig. 15a). Additionally, the ⟨100⟩ dislocations in CoZr (as well as in CoTi) have a much wider core than in NiAl (Table 6). Note, that the observation of an unusually wide core of ⟨100⟩ dislocations in CoTi was reported previously [39]. This feature of the dislocation structure will result in a low Peierls stress, high dislocation mobility and hence easy plastic relaxation which will prevent brittle fracture.

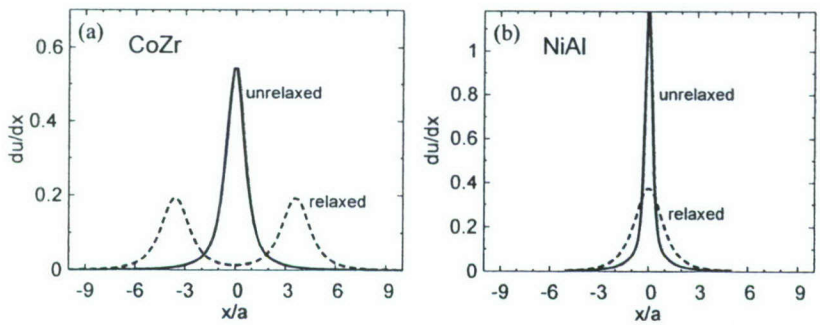

Figure 15: Core structure of the ⟨100⟩{011} screw dislocations in (a) CoZr and (b) NiAl.

Thus, the high ductility of CoZr is an intrinsic property and is connected with an anomalously low relaxed GSF energy near 1/2⟨100⟩{011} shear, which is also an indication of the phase instability of B2 CoZr. A detailed understanding of the mechanism of this instability will require further investigations. Due to the similarity of the electronic structure, we expect similar behavior for all Co-based intermetallics.

10. Dislocation core structure in B2 intermetallics CoZr and NiAl: large scale ARM with ab initio parametrization.

The calculations within the planar PN model presented above allowed us to identify the important features of the dislocation core structure in CoZr. However, the PN model could not explain the temperature yield stress anomaly, which is related to the existence of at least two (mobile and sessile) core structures; therefore, a consideration of the dislocation structure beyond the scope of 2D PN model is necessary.

To make clear the conditions for the appearance of the non-planar dislocation core we investigated the structure of ⟨100⟩ dislocations in B2 CoZr and NiAl in the framework of a combined approach including the atomic row model (ARM) for screw dislocations with *ab initio* parameterization of the interatomic row interaction energy. This approach was previously successfully applied to modeling the alloying effect on the dislocation structure in bcc Mo and explaining the main trends in SSS phenomena [23],[29]. To describe the dislocation structure in B2 intermetallics, we have generalized this approach by taking into account (i) the geometry of the packing of atomic rows in B2 type alloys and (ii) three contributions $\Phi_{AB}(u)$, $\Phi_{AA}(u)$, and $\Phi_{BB}(u)$ to the interatomic row potential originating from the interaction between atomic rows with atoms of different type (A–B, A–A and B–B, respectively).

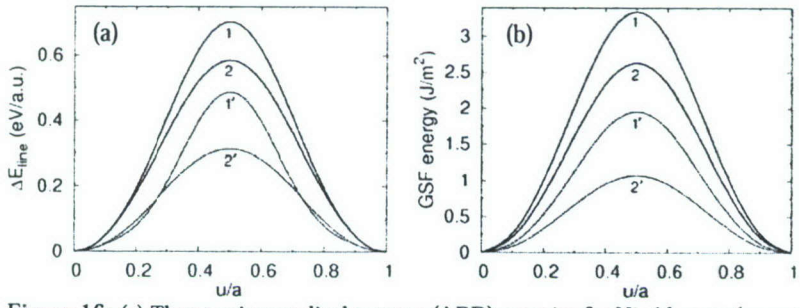

Figure 16: (a) The atomic row displacement (ARD) energies for Ni, Al–rows (curves 1, 2) and for Co, Zr–rows (curves 1 , 2) in NiAl and CoZr; (b) unrelaxed GSF energy for ⟨100⟩{001} and ⟨100⟩{011} shear (curves 1, 1 and 2, 2 , correspondingly) in NiAl (1, 2) and CoZr (1 , 2).

The dependencies of $\Phi_{AB}(u)$, $\Phi_{AA}(u)$, and $\Phi_{BB}(u)$ were determined by fitting to the atomic row displacement energies ΔE^{A}_{row} and ΔE^{B}_{row} along ⟨001⟩ with the GSF energy for ⟨100⟩{011} shear. Results of calculations of ΔE^{A}_{row} , ΔE^{B}_{row} and GSF energies by FLAPW [4] method are shown in Fig. 16 for CoZr and NiAl. While ARD energies for Ni and Al rows in NiAl are close, the ARD energy for Zr row is much smaller in comparison with the Co row in CoZr (Fig.16(a)); a similar trend takes place for the GSF energy in {001} and {011} planes (Fig.16(b)).

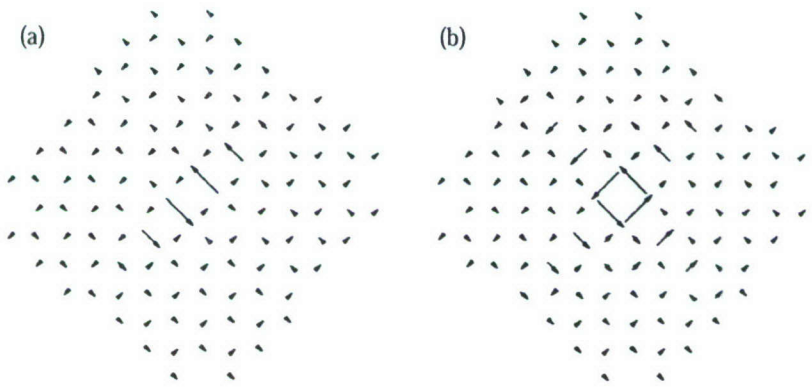

Figure 17: The planar (a) and non-planar (b) cores of the ⟨100⟩ screw dislocation in CoZr.

Using the ARM with *ab initio* determined $\Phi_{AB}(u)$, $\Phi_{AA}(u)$, and $\Phi_{BB}(u)$ potentials, we found that screw dislocations in NiAl have a compact core, which agrees with our previous theoretical results [35] and experimental observation [41]. For CoZr, we obtained an unusual result: two types of dislocation structures with planar and non-planar cores are possible; these are shown in Fig. 17 in the form of relative displacement maps. The planar core structure is in agreement with previous *ab initio*

PN calculations for unrelaxed GSF and correspond to the splitting of the ⟨100⟩ dislocation according to the $\mathbf{b} = \mathbf{b}/2 + \mathbf{b}/2$ scheme on the {011} plane. A non-planar core is formed by splitting on the two crossing {011} planes which results in a loss of mobility for this type of dislocation. The non-planar core originates from highly different GSF energies in {001} and {011} planes – a common feature for all Co-based B2 intermetallics.

Finally, an increase in temperature can lead to a loss of dislocation mobility due to planar–non-planar core transformation which will result in a positive $\sigma_y(T)$ dependence. Thus, our calculations explain this feature of mechanical behavior of B2 CoZr and allow us to conclude that the yield stress anomaly is an intrinsic property of the Co-based intermetallic alloys, rather than an extrinsic effect as was previously proposed [42].

References

[1] Y.F. Gu, Y. Yamabe-Mitarai, S. Nakazawa, and H. Harada, Materials Science and Engineering A, Vol. 329, pp.262-267 (2002).

[2] Yu.N. Gornostyrev, M.I. Katsnelson, N.I. Medvedeva, O.N. Mryasov, A.J. Freeman, and A.V. Trefilov, Physical Review B, Vol. 62, pp. 7802-7808 (2000).

[3] J.R. Rice and R. Thomson, Philosophical Magazine, Vol. 29, pp. 73-97 (1974).

[4] E. Wimmer, H. Krakauer, M. Weinert, and A.J. Freeman, Physical Review B, Vol. 24, pp. 864-875 (1981).

[5] Y. Yamabe-Mitarai, Y. Ro, T. Maruko, and H. Harada, Metallurgical and Materials Transactions A, Vol. 29, pp. 537-549 (1998).

[6] Y. Yamabe-Mitarai, Y. Koizumi, H. Murakami, Y. Ro, T. Maruko, and H. Harada, Scripta Materialia, Vol. 36, pp. 393-398 (1997).

[7] Y. Yamabe-Mitarai, M.-H. Hong, Y. Ro, and H. Harada, Philosophical Magazine Letters, Vol. 79, pp. 673-682 (1999).

[8] O.Yu. Kontsevoi, Yu.N. Gornostyrev, A.F. Maksyutov , K.Yu. Khromov, and A.J. Freeman, Metallurgical and Materials Transactions A, Vol. 36, pp. 559-566 (2005).

[9] O.N. Mryasov, Yu.N. Gornostyrev, M. van Schilfgaarde, and A.J. Freeman, Acta Materialia, Vol. 50, pp. 4545-4554 (2002).

[10] D. Siebörger, H. Brehm, F. Wunderlich, D. Möller, and U. Glatzel, Zeitschrift für Metalkunde, Vol. 92, pp. 58-61 (2001).

[11] Y. Yamabe-Mitarai, Y. Ro, T. Maruko, T. Yokokawa, and H. Harada, in *Structural Intermetallics 1997*, edited by M.V. Nathal, R. Darolia, C.T. Liu, P.L. Martin, D.B. Miracle, R. Wagner, and M. Yamaguchi, TMS, Warrendale, 1997, p. 805.

[12] G. Bruno, G. Schumacher, H.C. Pinto, and C. Schulze, Metalurgical and Materials Transactions A, Vol. 34, pp.193-197 (2003).

[13] R. Schmidt and M. Feller-Kniepmeier, Scripta Metallurgica et Materialia, Vol. 29, pp. 863-868 (1993).

[14] S. Baroni, S. de Gironcoli, A. Dal Corso, and P. Giannozzi, Reviews of Modern Physics, Vol. 73, pp. 515-562 (2001).

[15] W.D. Klopp, Journal of Less-Common Metals, Vol. 42, pp. 261-278 (1975).

[16] E. Pink and R.J. Arsenault, Materials Science, Vol. 24, pp. 1-50 (1979).

[17] J.R. Stephens and W.R. Witzke, Journal of Less-Common Metals, Vol. 41, pp. 265-282 (1975).

[18] T.E. Mitchell, P.M. Anderson, M.I. Baskes, S.P. Chen, R.G. Hoagland, and A. Misra,

Philosophical Magazine, Vol. 83, pp. 1329-1346 (2003).
[19] M. Methfessel and M. Scheffler, Physica B, Vol. 172, pp. 175-183 (1991).
[20] C. Woodward and S.I. Rao, Physical Review Letters, Vol. 88, art. No. 216402 (2002).
[21] A.H.W. Ngan, Philosophical Magazine, Vol. 79, pp. 1697-1720 (1999).
[22] S. Takeuchi, Philosophical Magazine A, Vol. 39, pp. 661-671 (1979).
[23] N.I. Medvedeva, Yu.N. Gornostyrev, and A.J. Freeman, Physical Review Letters, Vol. 94, Art. No. 136402 (2005).
[24] D. Shindo, M. Yoshida, B.T. Lee, T. Takasugi, and K. Hiraga, Intermetallics, Vol. 3, pp. 167-171 (1995).
[25] C. Woodward and S.I. Rao, Physical Review Letters, Vol. 88, Art. No. 216402 (2002).
[26] E. Pink and R.J. Arsenault, Materials Science, Vol. 24, pp. 1-50 (1979).
[27] S. Nemat-Nasser and A. Kapoor, International Journal of Plasticity, Vol. 17, pp.1351-1366 (2001).
[28] S.R. Chen and G.T. Gray, Metallurgical and Materials Transactions A, Vol. 27, pp. 2994-3006 (1996).
[29] N.I. Medvedeva, Yu.N. Gornostyrev, and A.J. Freeman, Physical Review B, Vol. 72, No. 10, Art. No. 134107 (2005).
[30] R.W. Buckman, in Proceeding of International Conference "Rhenium and Rhenium alloys", edited by B.D. Bryskin (TMS, Warrendale, PA, 1997), pp. 629-634.
[31] W.D. Klopp, Recent Developments in Chromium and Chromium Alloys, NASA Technical Reports, 70N20869, 1970.
[32] N.I. Medvedeva, Yu.N. Gornostyrev, and A.J. Freeman, Acta Materialia, Vol. 50, No. 10, pp. 2471-2476 (2002).
[33] Yu.N. Gornostyrev, M.I. Katsnelson, and A.V. Trefilov, in Proceeding of International Conference "Rhenium and Rhenium alloys", edited by B.D. Bryskin (TMS, Warrendale, PA, 1997), pp. 681-687.
[34] A. Gorbunov, A.A. Levin, A. Mensch, D.C. Meyer, A. Tselev, P. Paufler, W. Pompe, and D. Eckert, Applied Surface Science B, Vol. 97, pp. 475-480 (2002).
[35] N.I. Medvedeva, O.N. Mryasov, Yu. N. Gornostyrev, D.L. Novikov, and A.J. Freeman, Physical Review B, Vol. 54, pp. 13506-13514 (1996).
[36] K. Gschneidner, A. Russel, A. Pecharsky, J. Morris, Z. Zhang, T. Lograsso, D. Hsu, C.H.C. Lo, Y. Ye, A. Slager, and D. Kesse, Nature materials, Vol. 2, pp. 587-590 (2003).
[37] T. Yamaguchi, Y. Kaneno, and T. Takasugi, Scripta Materialia, Vol. 52, pp. 39-44 (2005).
[38] T. Takasugi, S. Hanada, M. Yoshida, and D. Shindo, Philosophical Magazine A, Vol. 71, pp. 347-358 (1995).
[39] D. Shindo, M. Yoshida, B.T. Lee, T. Takasugi, and K. Hiraga, Intermetallics, Vol. 3, pp. 167-171 (1995).
[40] Y.M Sun, G.E. Beltz, and J.R. Rice, Materials Science and Engineering A, Vol. 170, pp. 67-85 (1993).
[41] M.J. Mills and D.B. Miracle, Acta Materialia, Vol. 41, pp. 85-95 (1993).
[42] M. Wittmann and I. Baker, Materials Science and Engineering A, Vol. 329-331, pp. 206-212 (2002).

Personnel Supported

Dr. Oleg Y. Kontsevoi	Senior Research Associate, Northwestern University, Evanston, IL
Prof. Yuri N. Gornostyrev	Visiting Research Scientist from Institute of Metal Physics, Ekaterinburg, Russia
Dr. Nadezhda I. Medvedeva	Visiting Research Scientist from Institute of Solid State Chemistry, Ekaterinburg, Russia

Publications

1. "Negative yield stress temperature anomaly and structural instability of Pt_3Al", Yu.N. Gornostyrev, O.Yu. Kontsevoi, A.F. Maksyutov, A.J. Freeman, M.I. Katsnelson, A.V. Trefilov, and A.I. Lichtenshtein, Physical Review B, Vol. 70, No.1, Art. No. 014102 (2004).
2. "Interfacial strength and misfit dislocations in eutectic composites: NiAl/Mo", N.I. Medvedeva, Yu.N. Gornostyrev, O.Yu. Kontsevoi, and A.J. Freeman, Acta Materialia, Vol. 52, No. 3, pp. 675-682 (2004).
3. "Relation of Phase Stability and Mechanical Properties of Intermetallic Alloys: Modern Computational Materials Science Approach", A.J. Freeman, O.Yu. Kontsevoi, and Yu.N. Gornostyrev, TMS Letters, Vol. 1, No.2, pp. 40-41 (2004).
4. "Dislocation structure, phase stability and yield stress behavior of $L1_2$ intermetallics: Ir_3X (X = Ti, Zr, Hf, V, Nb, Ta)", O.Yu. Kontsevoi, Yu.N. Gornostyrev, A.F. Maksyutov, K.Yu. Khromov, and A.J. Freeman, Metallurgical and Materials Transactions A, Vol. 36, pp. 559-566 (2005).
5. "Modeling the dislocation properties and mechanical behavior of Ir, Rh, and their refractory alloys", O.Yu. Kontsevoi, Yu.N. Gornostyrev, and A.J. Freeman, JOM, Vol. 57, No. 3, pp. 44-47 (2005).
6. "Electronic origin of solid solution softening in bcc molybdenum alloys", N.I. Medvedeva, Yu.N. Gornostyrev, and A.J. Freeman, Physical Review Letters, Vol. 94, Art. No. 136402 (2005).
7. "Solid solution softening in bcc Mo alloys: Effect of transition-metal additions on dislocation structure and mobility", N.I. Medvedeva, Yu.N. Gornostyrev, and A.J. Freeman, Physical Review B, Vol. 72, Art. No. 134107 (2005).
8. "Dislocation structure, phase stability and yield stress behavior of ultra-high temperature $L1_2$ intermetallics: combined first-principles-Peierls-Nabarro approach", O.Yu. Kontsevoi, Yu.N. Gornostyrev, and A.J. Freeman, in Integrative and Interdisciplinary Aspects of Intermetallics, edited by M.J. Mills et al. (MRS Symposium Proceedings, Warrendale, PA, 2005), Vol. 842, pp. 511-516.
9. "The role of thermal expansion and composition changes in the temperature dependence of the lattice misfit in two-phase γ/γ' superalloys, Yu.N. Gornostyrev, O.Yu. Kontsevoi, K.Yu. Khromov, M.I. Katsnelson, and A.J. Freeman, Scripta Materialia, Vol. 56, pp. 81-84 (2007).
10. "Solid solution softening and hardening in the group-V and group-VI bcc transition metals alloys: First principles calculations and atomistic modeling", N.I. Medvedeva,

Yu.N Gornostyrev, and A.J. Freeman, Physical Review B, Vol. 76, Art. No. 212104 (2007).

11. "Role of thermal expansion and redistribution of components on the temperature dependence of the lattice misfit in γ/γ', Yu.N. Gornostyrev, O.Yu. Kontsevoi, and A.J. Freeman, in Advanced Intermetallic-Based Alloys, edited by J. Wiezorek et al. (MRS Symposium Proceedings, Warrendale, PA, 2007), Vol. 980, pp. 505-510.
12. "First principles calculations of thermal expansion and the temperature dependence of the lattice misfit parameter in two-phase refractory superalloys: Ir/Ir_3Nb and Pt/Pt_3Al", K.Yu. Khromov, Yu.N. Gornostyrev, O.Yu. Kontsevoi, A.F. Maksyutov, M.I. Katsnelson, A.I. Lichtenstein, A.V. Trefilov, and A.J. Freeman, Physical Review B (submitted).
13. "Electronic mechanism of strong "chemical interactions" of transition metal impurities with edge and screw dislocations: NiAl", O.Yu. Kontsevoi, Yu.N. Gornostyrev, and A.J. Freeman, Physical Review B (submitted).
14. "Effect of light impurities on the formation of A15 phase in chromium", N.I. Medvedeva, O.Yu. Kontsevoi, Yu.N. Gornostyrev, and A.J. Freeman, Physical Review B (submitted).

Presentations

1. "Modern computational materials science: the problem of alloy phase stability", A.J. Freeman, TMS Annual Meeting, March 14-18, 2004, Charlotte, NC.
2. "Dislocation structure and mechanical behavior of Ir-based γ' alloys", O.Yu. Kontsevoi, Yu.N. Gornostyrev, A.F. Maksyutov, and A.J. Freeman, TMS Annual Meeting, March 14-18, 2004, Charlotte, NC.
3. "Dislocation structure and mechanical behavior of Ir_3X $L1_2$ alloys: ab-initio investigation", O.Yu. Kontsevoi, A.J. Freeman, Yu.N. Gornostyrev, A.F. Maksyutov, and K.Yu. Khromov, American Physical Society Meeting, March 22-26, 2004, Montreal, QC, Canada.
4. "First principles study of solid solution softening in Mo alloys", N.I. Medvedeva, Yu.N. Gornostyrev, and A.J. Freeman, American Physical Society Meeting, March 22-26, 2004, Montreal, QC, Canada.
5. "Thermal expansion and lattice misfit in two-phase superalloys", Yu.N. Gornostyrev, O.Yu. Kontsevoi, A.J. Freeman, K.Yu. Khromov, A.F. Maksyutov, A.V. Trefilov, M.I. Katsnelson, and A.I. Lichtenstein, American Physical Society Meeting, March 22-26, 2004, Montreal, QC, Canada.
6. Dislocation structure, phase stability and yield stress behavior of ultra-high temperature $L1_2$ intermetallics: combined first-principles-Peierlsl-Nabarro approach", O.Yu. Kontsevoi, Yu.N. Gornostyrev, and A.J. Freeman, MRS Fall Meeting, November 29-December 3, 2004, Boston, MA.
7. "Fundamental electronic structure characteristic and mechanical behavior of aerospace materials", A.J. Freeman, O.Yu. Kontsevoi, Yu.N. Gornostyrev, and N.I. Medvedeva, AFOSR Aerospace and Materials Sciences Program Review Meeting, August 16-18, 2004, Wintergreen, VA.
8. "Dislocation structure, phase stability and yield stress behavior of platinum group $L1_2$ intermetallics: combined ab-initio-Peierlsl-Nabarro model approach", O.Yu. Kontsevoi,

Yu.N. Gornostyrev, and A.J. Freeman, TMS Annual Meeting, February 13-17, 2005, San Francisco, CA.

9. "Effect of alloying on screw dislocation structure in Mo: atomistic modeling approach with ab-initio parametrization", N.I. Medvedeva, Yu.N. Gornostyrev, and A.J. Freeman, American Physical Society Meeting, March 21-25, 2005, Los Angeles, CA.
10. "Dislocation structure and mechanical behavior of Rh_3X $L1_2$ intermetallic alloys: combined ab-initio-Peierlsl-Nabarro model approach", O.Yu. Kontsevoi, Yu.N. Gornostyrev, and A.J. Freeman, American Physical Society Meeting, March 21-25, 2005, Los Angeles, CA.
11. "Effect of impurities on the electronic structure and stability of the A15 phase of chromium", N.I. Medvedeva, O.Yu. Kontsevoi, and A.J. Freeman, American Physical Society Meeting, March 21-25, 2005, Los Angeles, CA.
12. "Temperature dependence of the lattice misfit in γ/γ' superalloys: role of thermal expansion and composition changes", O.Yu. Kontsevoi, Yu.N. Gornostyrev, A.J. Freeman, and K.Yu. Khromov, American Physical Society Meeting, March 21-25, 2005, Los Angeles, CA.
13. "Fundamental electronic structure characteristic and mechanical behavior of aerospace materials", A.J. Freeman, O.Yu. Kontsevoi, Yu.N. Gornostyrev, and N.I. Medvedeva, AFOSR Metallic, Non-Metallic, and Ceramic Program Review Meeting, August 15-17, 2005, Sedona, AZ.
14. "Solid solution softening in Mo alloys: large-scale model with ab-initio parametrization", Yu.N. Gornostyrev, N.I. Medvedeva, and A.J. Freeman, TMS Annual Meeting, March 12-16, 2006, San Antonio, TX.
15. "Effect of antisite defects on the temperature dependence of the lattice misfit in γ/γ' alloys", O.Yu. Kontsevoi, Yu.N. Gornostyrev, and A.J. Freeman, TMS Annual Meeting, March 12-16, 2006, San Antonio, TX.
16. "Formation of topologically close packed impurity locked phases in Mo and Cr base alloys", N.I. Medvedeva, O.Yu. Kontsevoi, Yu.N. Gornostyrev, and A.J. Freeman, TMS Annual Meeting, March 12-16, 2006, San Antonio, TX.
17. "First-principles study of the Hume-Rothery electron concentration rule in Al-Cu-(Fe,Ru)-Si 1/1-cubic approximants", R. Asahi, O.Y. Kontsevoi, U. Mizutani, T. Takeuchi, and A.J. Freeman, American Physical Society Meeting, March 13-17, 2006, Baltimore, MD.
18. "Fundamental electronic structure characteristic and mechanical behavior of aerospace materials", A.J. Freeman, O.Yu. Kontsevoi, Yu.N. Gornostyrev, and N.I. Medvedeva, AFOSR Metallic Materials Program Review Meeting, November 1-3, 2006, Arlington, VA.
19. "Role of thermal expansion and redistribution of components in the temperature dependence of the lattice misfit in γ/γ' superalloys", O.Yu. Kontsevoi, Yu.N. Gornostyrev, and A.J. Freeman, MRS Fall Meeting, November 27-December 1, 2006, Boston, MA.
20. "Role of topologically close packed phase precipitates in ductilizing Cr-Re and Mo-Re alloys", O.Yu. Kontsevoi, N.I. Medvedeva, Yu.N. Gornostyrev, and A.J. Freeman, MRS Fall Meeting, November 27-December 1, 2006, Boston, MA.